lubricants

MDPI

Article

Impact of Brake Wear Particles on Eukaryotic Cell Viability and Associated Oxidative Stress Responses

Lina Trečiokaitė [1,*], Yurii Tsybrii [2], Oleksii Nosko [2] and Lina Ragelienė [1]

[1] Faculty of Natural Sciences, Vytautas Magnum University, LT-53361 Kaunas, Lithuania; lina.rageliene@vdu.lt
[2] Faculty of Mechanical Engineering and Ship Technology, Gdansk University of Technology, 80-233 Gdańsk, Poland; yurii.tsybrii@pg.edu.pl (Y.T.); oleksii.nosko@pg.edu.pl (O.N.)
* Correspondence: lina.treciokaite@vdu.lt

Abstract: In this study, the cytotoxic effects of brake wear particles (≥250 nm ceramic/ceramic wear particles (CCWPs) and ≤100 nm ceramic/steel wear particles (CSWPs)) and 100 nm iron (III) oxide ultrafine particles (IOUFPs) on human lung carcinoma (A549) and Chinese hamster ovary (CHO) cells were investigated. Cell viability was determined using the MTT and Calcein AM methods. Oxidative stress was assessed by measuring reactive oxygen species (ROS), intracellular reduced glutathione (GSH), and malondialdehyde (MDA) concentrations under exposure to the above particles in the concentration range of 10–80 μg/mL. The initial assessments of CCWPs and CSWPs on the cell viability were performed after a 4-h exposure but later extended to 24 h to investigate the time-dependent of the cell viability and oxidative stress. MTT and Calcein AM assays indicated that the A549 cells are less susceptible to CCWPs and CSWPs than the CHO cells when exposed for both 4 h and 24 h. This study highlights that oxidative stress induced by CCWPs, CSWPs, and IOUFPs is cell-specific. While CCWPs did not affect glutathione (GSH) levels in the CHO cells, it significantly reduced GSH levels in A549 cells, with the exception of 80 μg/mL. Both CCWPs and CSWPs increased the lipid peroxidation in both cell types; however, the A549 cells demonstrated lower sensitivity to these treatments.

Keywords: car brake wear particles; Fe_2O_3 ultrafine particles; viability; CHO; A549 cells; oxidative stress

Citation: Trečiokaitė, L.; Tsybrii, Y.; Nosko, O.; Ragelienė, L. Impact of Brake Wear Particles on Eukaryotic Cell Viability and Associated Oxidative Stress Responses. *Lubricants* **2024**, *12*, 449. https://doi.org/10.3390/lubricants12120449

Received: 20 September 2024
Revised: 2 December 2024
Accepted: 12 December 2024
Published: 16 December 2024

1. Introduction

Wear particles belong to traffic-related pollutants that originate from the wear of the brakes and tires of motor vehicles and roads [1,2]. Brake wear contributes up to 55% of fine particles for non-exhaust traffic emissions [3,4]. A passenger car is normally equipped with four brakes, each consisting of two brake pads and a disc. The brake pads are composed of various ingredients, which are often categorized as reinforcements, abrasives, lubricants, fillers, and binders [2,5]. The reinforcements (e.g., steel, carbon, and glass fibers) are added to the friction material formulation to provide the mechanical strength. The abrasives (e.g., aluminum and iron oxides, silicon dioxide, and zirconium oxide) change the friction and wear properties. The lubricants (e.g., graphite and copper sulfate) stabilize the friction properties, especially at high temperatures. The fillers (e.g., barite, calcite, and mica) fill in the space between the other ingredients and improve the manufacturability of the friction material. The binders (e.g., phenolic and silicone resins) ensure the structural integrity under thermomechanical loads [2].

When the brake pads and discs are worn off, wear particles are released to the environment and affect living organisms. The biological effect of particles depends on their size [6–9] and charge [10], surface coating [7,11,12], chemical nature [8,13], ionization constant [14], and pH of the medium [15,16]. For example, smaller 40–50 nm copper particles are more toxic [8,9] compared to larger micrometer-sized copper particles [17,18]. The penetration of wear particles into cells depends on the size and morphology of the particles

and the surface coverage. They can penetrate the plasma membrane of the cell or enter the cells through the active transport mechanism called endocytosis (phagocytosis and pinocytosis) [19]. The uptake of larger particles occurs by phagocytosis. The uptake of particles with a size from a few nanometers to hundreds of nanometers, on the other hand, takes place via pinocytosis [20–24].

At the molecular level, the formation of reactive oxygen species (ROS), hydrogen peroxide, anionic superoxide, and free hydroxyl radical, as well as hydroxyl anion, is a major mechanism by which nanomaterials trigger cellular responses [13,25] and cause the oxidative stress in cells [8,26]. Cell proliferation can be regulated by ROS levels. For example, when the intracellular ROS level is above a certain threshold, ROS inhibits the cell cycle, leading to increased cell necrosis and apoptosis [27,28]. Wear particles can also participate in ionization. There is evidence that metal ions react with hydrogen peroxide (H_2O_2) in the cytosol and in biological membranes and are the main target of the oxidative stress. The cell membrane, which is composed of polyunsaturated fatty acids, is a primary target for attacks by superoxide anions and H_2O_2, resulting in cell membrane damage [29–31]. H_2O_2, which is categorized as a non-radical ROS, can be converted into much more active other ROS derivatives under the influence of various compounds, including proteins, lipids, and enzymes. Metal cations released from wear particles bind to negatively charged phospholipids, thus altering the physical properties of the bilayer and favoring the initiation and propagation of lipid peroxidation reactions [31,32]. Malondialdehyde (MDA), propanal, hexanal, and other various aldehydes can be formed as secondary products during lipid peroxidation [31]. The practically non-toxic MDA is considered a presumptive biomarker for lipid peroxidation in living organisms and cultured cells [33,34]. On the other hand, the end products of lipid peroxidation (one of which is MDA) cause the protein damage by addition reactions with lysine amino groups, cysteine sulfhydryl groups, and histidine imidazole groups [35,36].

The studies on the influence of brake wear particles on the viability of cells have led to the controversial results. For example, Barosova et al. [37], Gasser et al. [38], and Puisney-Dakhli et al. [39] found no significant effects on the cell viability after exposure. In contrast, the studies by Alves et al. [40], Melzi et al. [41], and Puisney et al. [42] clearly demonstrated the particle cytotoxicity. In the mentioned studies, the concentration of particulate matter (PM) varies in a wide range from 150 to 400 ng/mL [40] to 2, 1, and 0.5 mg/mL [37]. Following Puisney et al. [42] with 25–50–100–150 μg/mL PM, the suspension concentration of 10–80 μg/mL is used in the present study. The studies on the effects of brake wear particles on the production of ROS have also shown contradictory results. Melzi et al. [41] and Puisey et al. [42] reported an increase in the ROS production after exposure, whereas Alves et al. [40], Barosova et al. [37], Gasser et al. [38], and Zhao et al. [43] did not observe this effect.

The aim of this study was to systematically investigate and compare the viability, ROS generation, and membrane effects of wear particles emitted from ceramic/ceramic and ceramic/steel brake friction pairs and Fe_2O_3 ultrafine particles on CHO and A549 cells.

2. Materials and Methods

Materials: We used 100 nm Fe_2O_3 ultrafine particles (IOUFP), Sigma-Aldrich, Eschenstrasse 5 D-82024 Taukirchen, Germany; ceramic brake pads commonly used in passenger cars in the Baltic countries; ≥250 nm ceramic/ceramic wear particles (CCWPs) generated by rubbing the ceramic brake pad samples against each other; and ≤100 nm ceramic/steel wear particles (CSWP) generated by rubbing the ceramic brake pad sample against a S235JR steel disc.

The wear particles were obtained using the experimental setup and procedure described in Tarasiuk et al. [44]. The pin samples had a diameter of 8 mm and a length of 8 mm. They were tested on a pin-on-disc tribometer against steel discs with a diameter of 60 mm and a thickness of 6.5 mm, at a sliding speed of 1.8 m/s and a contact pressure of 1 MPa. The temperature measured in the pin sample did not exceed 100 °C during the

test. A clean chamber was built around the friction pair of the tribometer to eliminate the external sources of particles. The clean chamber was supplied with filtered and dried air at its inlet. The friction between the pin and disc samples led to the emission of wear particles into the air. The airflow in the clean chamber transported the wear particles to the outlet of the clean chamber, where they were sampled by a cascade impactor. The cascade impactor provided a three-stage classification and collection of the wear particles according to their aerodynamic diameters. The upper stage, with a cut point of 10 μm, collected >10 μm particles. These larger particles are not inhalable and are not considered in this study. The middle stage, with a cut point of 2.5 μm, collected 2.5–10 μm particles. Finally, the lower stage, with a cut point of 1 μm, collected 1–2.5 μm particles. At each stage, the wear particles were collected on an aluminum substrate.

The cell line Chinese hamster ovary (CHO) and the cell line Human lung cancer (A549), Merck SA.

Reagents: 3-(4,5-dimethylthiazol-2-yl)-2,5-diphenyl-2H-tetrazolium bromide (MTT), Roth; N,N′-[[3′,6′-bis(acetyloxy)-3-oxospiro[isobenzofuran-1(3H),9′-[9H]xanthene]-2′,7′-diyl]bis(methylene)]bis[N-[2-[(acetyloxy)methoxy]-2-oxoethyl]]-glycine,1,1′-bis [(acetyloxy) methyl] ester (Calcein AM), Cayman; dimethyl sulfoxide (DMSO), Sigma-Aldric; 2-propanone (Acetone), Sigma-Aldrich; phosphate-buffered saline (PBS), Roth; 2′, 7′-dichlorodihydrofluorescein diacetate (DCF-DA), TRC Canada; hydrogen peroxide (H_2O_2), Chempur; Propanedial (Malondialdehyde) (MDA), Sigma-Aldric; Tris-HCl, NaCl, Na_2EDTA, Triton X-100, sodium pyrophosphate solution (cell lysis buffer), Acros Organics; trichloroacetic acid (TCA), AppliChem; 2-thiobarbituric acid (TBA), Acros Organics; benzene-1, 2-dicarbaldehyde (phthalaldehyde), Sigma-Aldric; perchloric acid, Sigma-Aldric; Dulbecco's Modified Eagle Medium (DMEM), Cegrogen; Fetal Bovine Serum (FBS), Cegrogen; benzylpenicillin/streptomycin sulphate (penicillin/streptomycin) (P/S), Cegrogen; amphotericin B (AmphB), Cegrogen; RPMI medium (RPMI 1640), Roth; 2-Aminopentanedioic acid (L-Glutamic acid) (L-Glu), Roth.

The stock solution of particles: Suspensions of CCWPs, CSWPs, and IOUFPs were prepared at 0.1 g/mL in autoclaved deionized water. CCWP suspensions were sonicated for 2 h and centrifuged at 7000 rpm for 10 min. CSWP and IOUFP suspensions were sonicated for 0.5 h and centrifuged at 7000 rpm for 10 min [39,40]. The stock solutions were stored in the dark at +4 °C and were vortexed before each use.

Eukaryotic cells cultivation: CHO cells were cultured in a sterile DMEM cell culture medium with 10% FBS, 1% P/S, and 1% AmphB. The temperature in the incubator was 37 °C, with 5% CO_2 and a humidity of 80%. The incubation lasted between 4 and 5 days. A549 cells were cultured in a sterile RPMI 1640 cell culture medium with 10% FBS, 1% P/S, 1% AmphB, and 1–3% L-Glu, at an incubator temperature of 37 °C, a CO_2 content of 5%, and a humidity of 80%. The incubation lasted between 6 and 7 days.

Cell incubation with IOUFP, CCWP, and CSWP suspension: Approximately 10,000 cells/mL in the exponential growth phase were seeded in a flat-bottomed 96-well black/transparent polystyrene-coated plate and incubated for 24 h at 37 °C in a 5% CO_2 incubator. The prepared series of 10, 20, 40, and 80 μg/mL of IOUFP, CCWP, and CSWP in the medium were added to the plate (100 μL). The incubation time with the CSWP, CCWP, and IOUFP suspensions in the cell viability/cytotoxicity studies was 4 or 24 h. The investigation of the ROS formation, lipid peroxidation, and intracellular reduced GSH was performed after 24 h of incubation with CSWP, CCWP, and IOUFP suspensions.

Cell viability/cytotoxicity studies were performed under the following conditions. The cytotoxicity of CSWP, CCWP, and IOUFP was analyzed with the MTT assay according to ISO 19007:2018 [45]. After the incubation of the cells with CSWP, CCWP, and IOUFP for 4 or 24 h, the cell growth medium in each well was replaced with 100 μL MTT (0.2 mg/mL). The subsequent incubation was carried out for 4 h. The formation of formazan crystals was observed after 4 h in each well. These formazan crystals were dissolved in 50 μL acetone, and the OD was immediately measured in a microplate reader (TECAN microplate reader)

at a wavelength of 535 nm. The cells incubated in the absence of particles were used as a control.

For the **cell viability study**, a 1 mM Calcein AM solution was prepared in DMSO [46]. The cell growth medium was replaced in each well with 100 µL Calcein AM solution (5 µM in PBS (pH 7.4)) after 4 or 24 h of the incubation with CSWPs, CCWPs, and IOUFPs. The subsequent incubation was carried out for 1 h. Then, 50 µL PBS was added to each well, and the plates were immediately read in a microplate reader (TECAN microplate reader) with an excitation wavelength of 490 and an emission wavelength of 535 nm. The cells incubated in the absence of particles were used as a control.

The evaluation of the **ROS generation** was performed under the following conditions. The cell growth medium was changed in each well with 100 µL 10 µM DCF-DA after incubating the cells for 24 h in a medium without phenol red at 37 °C for 30 min in the dark [47]. The cells were washed twice with PBS. Then, 50 µL of PBS was added to each well, and the plates were immediately read in a microplate reader (TECAN microplate reader), with an excitation wavelength of 485 and an emission wavelength of 535 nm. The cells incubated in the absence of particles were used as a control. The ROS generation by H_2O_2 (100 µM) was used as a positive control.

The content of **intracellular reduced glutathione (GSH)** was determined with o-phthaldialdehyde [48]. After the treatment, the cells were lysed with 100 µL of 1% perchloric acid for 10 min on ice. Then, 10 µL cell lysates, KH_2PO_4/EDTA buffer, and o-phthaldialdehyde (1 mg/mL) were added to 96-well black plastic plates and incubated for 0.5 h at room temperature in the dark. The fluorescence intensity was measured using the microplate spectrofluorometer (TECAN microplate reader) at the excitation and emission wavelengths of 350 and 420 nm, respectively.

Lipid peroxidation was determined using the malondialdehyde (MDA) method [48,49]. The cells were cultured as described above. A 0.1 mL cell suspension was washed with PBS at 4 °C. The cell pellets were then lysed in cell lysis buffer (1 × 20 mM Tris-HCl (pH 7.5), 150 mM NaCl, 1 mM Na_2EDTA, 1% Triton X-100, and 2.5 mM sodium pyrophosphate). After the centrifugation (15,000× *g* for min at 4 °C), the supernatant (cell suspension) was kept on ice, and 1.9 mL 0.1 M sodium phosphate buffer (pH 7.4) was incubated at 37 °C for 1 h. After the incubation, the mixture was precipitated with 5% TCA and centrifuged (2300× *g* for 15 min at room temperature) to collect the supernatant. Further, 1.0 mL of 1% TBA was added to the supernatant and placed in boiling water for 15 min. After cooling to room temperature, the absorbance of the solution was measured at 532 nm, using a TECAN microplate reader.

For the **statistical analysis**, all data are means ± standard deviation (SD), one-way analysis of variance (ANOVA) of the least 3 replicates, $n = 3$, * $p < 0.05$, ** $p < 0.01$, and *** $p < 0.001$ compared to the control group (viability of cells without exposure of particles 100%): (a) significant difference as compared with CCWP between cell CHO and A549 lines at $p < 0.05$; (b) significant difference as compared with CSWP between cell CHO and A549 lines at $p < 0.05$; and (c) significant difference as compared with IOUFP between cell CHO and A549 lines at $p < 0.05$.

3. Results

In this study, the cytotoxic effects of ceramic/ceramic wear particles (CCWPs), ceramic/steel wear particles (CSWPs), and iron (III) oxide ultrafine particles (IOUFPs) are investigated using the same concentration suspensions on the cells of two lines.

The first line was human lung adenocarcinoma cells (A549), which are frequently used in research due to the ease of their cultivation and relevance to lung diseases [50]. A549 cells have a typical epithelial cell membrane, form tight junctions, and express epithelial markers [50]. Due to their membrane composition and the expression of various receptors, they respond to a range of stimuli, including cytokines and growth factors [51].

The second line was Chinese hamster ovary (CHO) cells. Type II cells have characteristic ultrastructural features, including a cuboidal shape, an expanded cytoplasm with

a rough endoplasmic reticulum, tight junctions, and lamellar bodies [52]. CHO cells can produce proteins with complex bioactive post-translational modifications (PTMs) similar to those found in humans [53]. Glycosylation of CHO glycoprotein is closer to that in human cells due to the absence of immune galactose–galactose epitopes in CHO cells [54].

3.1. Impact of Ceramic/Ceramic and Ceramic/Steel Wear Particles and Iron (III) Oxide Ultrafine Particles on the Viability of A549 and CHO Cells

Considering the mechanical properties, durability, and popularity on the domestic market, ceramic brake pads were selected for this study. Despite the growing interest in the toxicity of brake pad materials, the governing mechanisms are still poorly understood [55]. The viability of CHO and A549 cells was investigated using the MTT and Calcein AM methods.

The effects of the suspensions of CCWP, CSWP (Figure 1A), and IOUFP (Figure 1B) on the viability of CHO and A549 cells were determined using the MTT assay after 4 h exposure as described in Section 2.

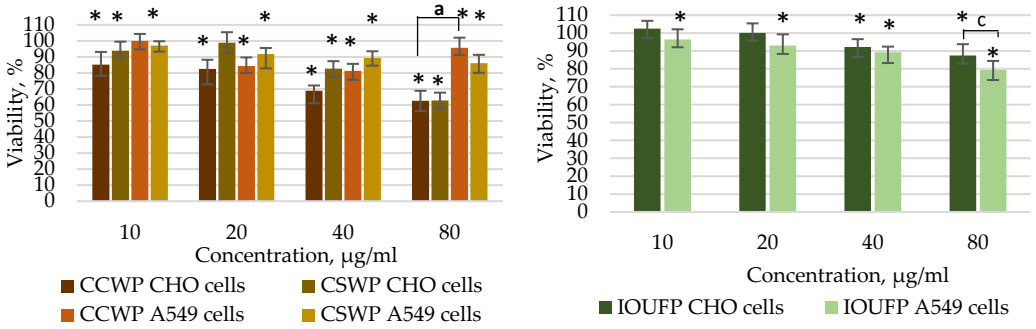

(**A**) (**B**)

Figure 1. Effect of the CCWP, CSWP (**A**), and IOUFP (**B**) suspensions for 4 h on the viability of CHO and A549 cells determined by the MTT method. Data are mean ± SD of at least 3 replicates, $n = 3$, * $p < 0.05$, compared to the control group (viability of cells without exposure of particles 100%): (a) significant difference as compared with CCWP between cell CHO and A549 lines at $p < 0.05$; (b) significant difference as compared with CSWP between cell CHO and A549 lines at $p < 0.05$; and (c) significant difference as compared with IOUFP between cell CHO and A549 lines at $p < 0.05$.

An exposure to a 10 µg/mL CCWP suspension resulted in a 15% decrease in the CHO cell viability compared to the control group that was not exposed to particles. A significant decrease in the cell viability, reaching approximately 31%, was observed when the CCWP concentration in the suspension was increased fourfold. The subsequent doubling of the concentration led to an additional decrease in the CHO cell viability. CHO cells exhibited a significant decrease in the viability when exposed to CSWPs at the concentrations of 40 and 80 µg/mL. After the exposure to a 40 µg/mL CSWP suspension, the viability of CHO cells decreased by 17%. Doubling the concentration to 80 µg/mL resulted in a 37% decrease in the viability compared to the control group.

A549 cells showed a lower sensitivity to CCWPs compared to CHO cells. Increasing the CCWP concentration from 10 to 20 µg/mL reduced the viability of A549 cells by 15.7%. A further increase in the CCWP suspension concentration to 40 µg/mL resulted in a decrease in viability to about 3%. Interestingly, when the CCWP concentration was increased to 80 µg/mL, the viability increased to 14.4%. Thereby, A549 cells were less sensitive to the effects of larger CCWPs and compared to CHO cells.

In the study [56], it was shown that iron has the highest concentration among all metals in the brake-pad composition. Therefore, Fe_2O_3 ultrafine particles with a stable oxidation state of the iron were chosen in the present study for investigating the effect of iron on the cell viability.

CHO cells showed no change in proliferation when exposed to the IOUFP suspensions at a concentration of 10 or 20 µg/mL. However, increasing the concentration twofold and fourfold led to a decrease in the viability of about 8% and 12%, respectively. In contrast, the A549 cell line showed a decrease in proliferation of approximately 3.6% at 10 µg/mL, with a small variation at 10 and 20 µg/mL. At 80 µg/mL, the proliferation of A549 cells was reduced by about 20%.

Both CHO and A549 cell lines showed a reduced viability with increasing concentrations of CCWPs and CSWPs, as determined by MTT over a short period of 4 h. The viability of A549 cells was less affected by higher CCWP and CSWP concentrations than CHO cells. IOUFPs had a dose-dependent effect on the viability of both cells. CHO cells were more resistant to the main effects of the metal than A549 cells.

The Calcein AM method was used to compare the effects of CCWPs, CSWPs, and IOUFPs on the cell viability under similar conditions. Figure 2A shows that the exposure to a 10 µg/mL CCWP suspension decreased the CHO cell viability by 7.6%. Doubling the concentration to 20 µg/mL led to a further decrease in the viability to 17%. A significant decrease to 22.8% in the viability was observed when the cells were exposed to 80 µg/mL of CCWPs compared to the control group. Similarly, the viability of CHO cells after 4 h of exposure to the 10 µg/mL CSWP suspension decreased by 7.3%. Doubling the concentration to 20 µg/mL led to an additional 5% decrease in the viability. Exposure to the 80 µg/mL suspension led to a significant decrease of 19.6% in the viability compared to the control group.

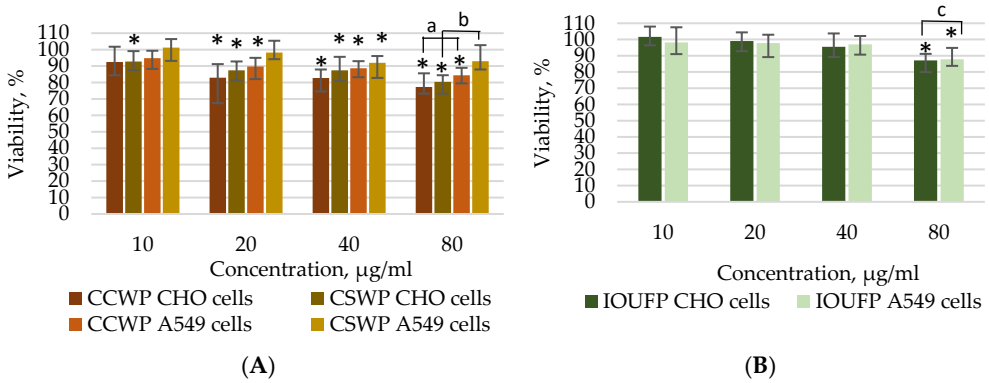

Figure 2. Effect of the CCWP, CSWP (**A**), and IOUFP (**B**) suspensions for 4 h on the viability of CHO and A549 cells determined by the Calcein AM method. Data are mean ± SD of at least 3 replicates, $n = 3$, * $p < 0.05$, compared to the control group (viability of cells without exposure of particles 100%): (a) significant difference as compared with CCWP between cell CHO and A549 lines at $p < 0.05$; (b) significant difference as compared with CSWP between cell CHO and A549 lines at $p < 0.05$; and (c) significant difference as compared with IOUFP between cell CHO and A549 lines at $p < 0.05$.

A549 cells showed a lower sensitivity to CCWP particles compared to CHO cells, as shown by the results of the MTT assay in Figure 1A. The decrease in the A549 cell viability was less than 10% for all concentrations, except for the highest concentration of 80 µg/mL, where a decrease of 15.7% was observed compared to the control group. An exposure to the 40 µg/mL CSWP suspension reduced the viability of A549 cells by about 8%. This effect took place even after doubling the concentration to 80 µg/mL.

The Calcein AM method showed no negative effects of IOUFP on the proliferation of CHO and A549 cells within 4 h. However, a slight decrease in the viability was observed: about 5% for CHO cells at 40 µg/mL and about 13% for both cell types at 80 µg/mL. These results can be explained by different mechanisms of action used in the MTT and Calcein AM methods to determine the cell viability. In the Calcein AM, a metabolically active, non-fluorescent dye is hydrolyzed by cellular esterase to produce a fluorescent form that is retained in the cytoplasm [57]. This dye does not affect the cell viability [58] and can easily penetrate living, intact cells [59]. The Calcein AM primarily measures cytosolic labile

iron rather than total cellular labile iron because the probe cannot penetrate the lysosomes, where a significant portion of the low-mass labile iron is sequestered. The Calcein AM is a strong iron chelator [60]. The MTT assay measures the extent of active metabolism within the affected cell population and provides information on the cell death or reduced proliferation compared to the control cells [10,61]. However, it is important to note that the MTT results only reflect the metabolic state of the cells and do not directly quantify the number of viable cells [54]. Furthermore, the sensitivity of the assay is limited due to the insolubility of the formazan product [29]. Consequently, an extrapolation of the metabolic activity data to cell number or overall viability may lead to inaccuracies.

Both CHO and A549 cells showed a reduced viability with increasing concentrations of CCWPs and CSWPs. The viability of A549 cells was less affected by higher CCWP and CSWP concentrations than the viability of CHO cells. IOUFPs showed a minimal effect on the cell viability at lower (10–20 µg/mL) concentrations, while a slight decrease was observed in both cell lines at higher concentrations (40–80 µg/mL). The viability of A549 cells exposed to 80 µg/mL CCWP, CSWP, and IOUFP suspensions for 4 h was significantly less affected compared to the viability of CHO cells.

The effects of CCWPs and CSWPs on the cell viability were evaluated using the MTT and Calcein AM assays (Figures 1 and 2) at an initial exposure time of 4 h. However, due to the complex multi-ingredient nature of brake pads and the time-dependent oxidation and ionization processes involved in the metal release, the exposure time was extended to 24 h for the subsequent experiments.

A 24-h exposure to CCWPs showed a concentration-dependent effect on the viability of CHO cells (Figure 3A). The most significant reductions in the viability (approximately 22% and 34% compared to the control group) were observed at the lowest concentrations of 10 and 20 µg/mL. Increasing the CCWP concentration did not lead to significant changes in the viability. An exposure of CHO cells to the 10 µg/mL CSWP suspension resulted in a 9.6% decrease in the viability. Doubling the concentration to 20 µg/mL did not lead to a further significant decrease. However, an exposure to the 40 µg/mL suspension led to a significant decrease of 25.8% in the viability compared to the control group. A further, albeit smaller, decrease of about 6% was observed when the concentration was doubled to 80 µg/mL.

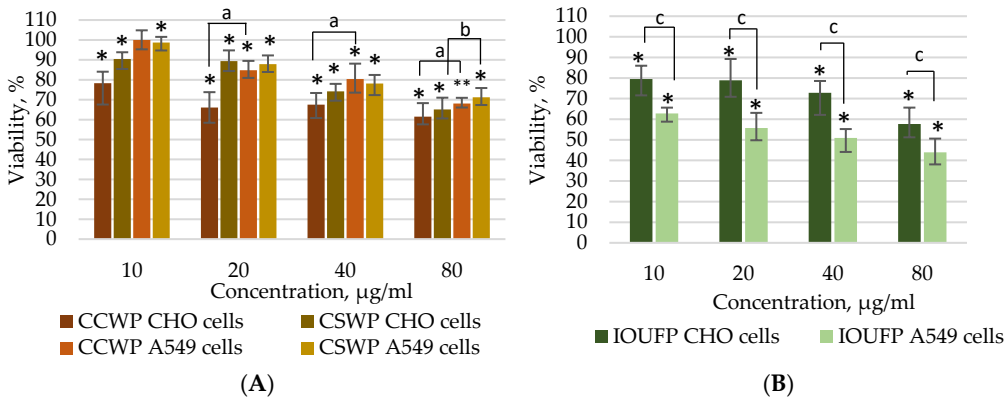

Figure 3. Effect of the CCWP, CSWP (**A**), and IOUFP (**B**) suspensions for 24 h on the viability of CHO and A549 cells determined by the MTT method. Data are mean ± SD of at least 3 replicates, $n = 3$, * $p < 0.05$, ** $p < 0.01$, compared to the control group (viability of cells without exposure of particles 100%): (a) significant difference as compared with CCWP between cell CHO and A549 lines at $p < 0.05$; (b) significant difference as compared with CSWP between cell CHO and A549 lines at $p < 0.05$; and (c) significant difference as compared with IOUFP between cell CHO and A549 lines at $p < 0.05$.

A549 cells showed a stronger resistance to the CCWP exposure than CHO cells. At a concentration of 10 µg/mL, no significant change was observed in the viability of A549

cells with the MTT method. However, doubling the concentration to 20 µg/mL resulted in a decrease in the A549 cell viability by approximately 15%. A significant decrease of 32% in the viability was observed at the highest concentration of 80 µg/mL. The viability of A549 cells after a 24-h exposure to nano-sized CSWPs followed a trend similar to larger CCWPs (Figure 3A). No significant effect was observed at the lowest concentration. However, at the highest concentration, a maximum decrease in the A549 cell viability of about 30% was observed. These findings correlate with the results on the viability of BEAS-2B bronchial cells [41] obtained with the MTT assay for 24 h of exposure to brake dust. It was found that the cell viability exhibits a statistically significant decline at a concentration of 50 µg/mL and a partial recovery at 100 µg/mL. This dose-dependent response suggests that the cell viability may stabilize at elevated concentrations, and this observation is in line with the results obtained in the present study. In the study by Alves et al. [40], the extracts derived from brake pads resulted in a reduction in the A549 cell viability by up to 80% at a concentration of 400 ng/mL. Figliuzzi et al. [62] reported that PM2.5 emissions from brake pads, particularly those characterized by a high copper content, elicit a dose-dependent decrease in the A549 cell viability. This effect was observed upon the exposure to increasing PM2.5 concentrations (1, 10, 100, 200, and 500 µg/mL) for 48 h, i.e., for a twice-longer exposure time compared to that in the present study.

An exposure of CHO cells to IOUFP suspensions with a concentration of 10 and 20 µg/mL led to a decrease of about 20% in the viability (Figure 3B). The most significant decrease to 42.3% was observed at a concentration of 80 µg/mL. A549 cells showed a stronger sensitivity in the viability for IOUFP. The 10 µg/mL CCWP suspension reduced the viability of A549 cells by 37%. This effect became stronger with the increasing concentration, culminating in the death of over 50% cells at 80 µg/mL. The viability of A549 cells was significantly lower following exposure to the IOUFP particles compared to the CHO cells across the tested concentration range of 10 to 80 µg/mL.

The Calcein AM assay revealed that most of the CHO cells did not survive for all concentrations of CCWP (Figure 4A). A549 cells were less sensitive for the prolonged exposure to CCWP: their viability decreased by 64% at 10 µg/mL, did not change considerably after doubling the concentration to 20 µg/mL, and finally decreased to 21% at 40 and 80 µg/mL.

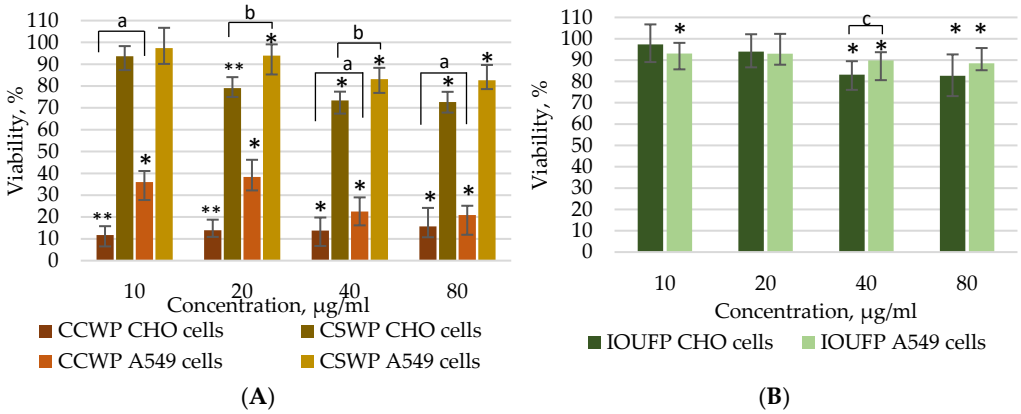

Figure 4. Effect of the CCWP, CSWP (**A**), and IOUFP (**B**) suspensions for 24 h on the viability of CHO and A549 cells determined by the Calcein AM method. Data are mean ± SD of at least 3 replicates, $n = 3$, * $p < 0.05$, ** $p < 0.01$, compared to the control group (viability of cells without exposure of particles 100%): (a) significant difference as compared with CCWP between cell CHO and A549 lines at $p < 0.05$; (b) significant difference as compared with CSWP between cell CHO and A549 lines at $p < 0.05$; and (c) significant difference as compared with IOUFP between cell CHO and A549 lines at $p < 0.05$.

Under the same conditions, CHO and A549 cells with CSWPs showed fewer negative effects on the cell viability, with a maximum decrease of about 20% in the cell viability for both lines after the exposure to 80 µg/mL CSWP (Figure 4A).

The viability of the A549 cells was approximately three-fold greater than that of the CHO cells when exposed to the CCWP suspension at a concentration of 10 and 20 μg/mL (Figure 4A). The significant difference in the viability between CHO and A549 cells was observed when exposed to elevated concentrations of 40 or 80 μg/mL. In comparing the effects of smaller CSWP particles on the cell viability, a statistically significant decrease in the viability was observed in CHO cells compared to A549 cells at suspension concentrations of 20 and 40 μg/mL.

IOUFPs showed only minimal effects on the viability of the CHO cells at concentrations up to 40 μg/mL. A reduction of approximately 17% in the CHO cell viability was observed following exposure to 40 or 80 μg/mL of IOUFPs. However, the A549 cells showed a stronger sensitivity to the IOUFPs (Figure 4B), as shown by the MTT assay (Figure 3B) after exposure to low concentrations of the IOUFP suspension. A 7% reduction in the A549 cell viability was observed upon exposure to 10 μg/mL of IOUFPs (Figure 4B). While a doubling of the concentration to 20 μg/mL did not cause a significant change, a two- or four-fold increase (40 or 80 μg/mL) led to a slight decrease of about 10%.

Comparing the impact of extended exposure time from 4 to 24 h on the viability of A549 and CHO cells highlighted the importance of choosing methods. After 24 h of exposure to 10 mg/mL CCWP suspension, the viability of CHO cells determined by the Calcein AM method was about eight times lower. Still, the viability determined by the MTT method was only 1.1 times lower. The data on the impact of the IOUFP suspension on the viability of CHO and A549 cells obtained by the MTT and Calcein AM methods differed. The MTT method indicated fewer metabolically active cells, suggesting more dead cells [54]. While there were consistent trends in the viability across different assay methods, the particle size and cell line led to some variability in the results. For a further investigation of the size-dependent effect, the literature sources [8,31] were analyzed, focusing on how the size and nature of the particles affect the mechanism of oxidative stress, which is a common effect of exposure to nanoparticles.

3.2. Impact of Ceramic/Ceramic and Ceramic/Steel Wear Particles and Iron (III) Oxide Ultrafine Particles on the Oxidative Stress in A549 and CHO Cells

The concentrations of ROS that ultimately lead to cell death are often far below the concentration that could be considered dangerous. In contrast, a single protein activated by ROS may be sufficient to initiate a genetic program leading to cell death [63]. ROS, including H_2O_2, are involved in the developmental control by inducing apoptosis and cell proliferation [33,56,64]. A 100 μM H_2O_2 solution was selected as a positive control for triggering the oxidative stress, as previous research has shown its effects on different cell lines at different exposure times [64].

The fluorescence intensity of the cell samples without CCWPs shows that CHO cells produce 11% more ROS than A549 cells under the conditions described in the Section 2 (Figure 5A). However, an exposure of A549 cells to the suspension showed a greater sensitivity to the oxidative stress. When CHO cells were exposed to the 10 μg/mL suspension of CCWP (using the same stock solution), 34% more ROS were generated than in A549 cells. Increasing the CCWP concentration from 40 to 80 μg/mL resulted in a 6% decrease in the ROS concentration in CHO cells. In contrast, CHO cells showed an increase in ROS production when exposed to a smaller-sized CSWP suspension. At a concentration of 10 μg/mL, the ROS levels in CHO cells were 21% higher than in the unexposed cells, and this increase reached 58% at a concentration of 80 μg/mL. A549 cells showed an increased sensitivity to CCWPs (Figure 5A). An exposure of the cells to the 10 μg/mL suspension resulted in a 53% increase in the ROS production compared to the control group. However, increasing the concentration by four or eight times had a less pronounced effect and resulted in ROS levels that were about 37% higher than those for the control group. In contrast to CHO cells, CSWPs did not significantly alter the oxidative stress in A549 cells. This observation is confirmed by a constant fluorescence intensity with increasing CSWP concentrations. While increasing concentrations of the IOUFP led to a reduced ROS formation in A549 cells

(Figure 5B), the opposite effect was observed in CHO cells. Regardless of the concentration, CHO cells consistently produced more ROS compared to the control group.

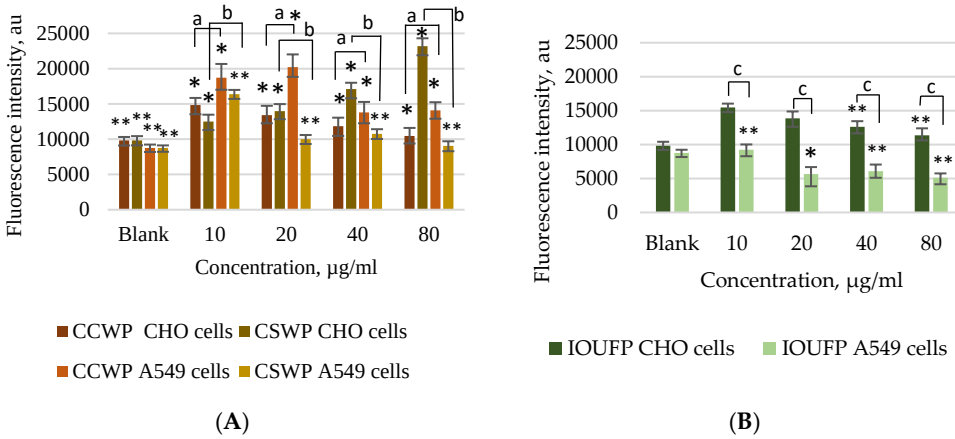

(**A**) (**B**)

Figure 5. Effect of the CCWP, CSWP (**A**), and IOUFP (**B**) suspension for 24 h on the ROS formation in the CHO and A549 cells. CHO had 30,000 fluorescence intensity (**A**,**B**), and A459 had 28,000 fluorescence intensity (**A**,**B**), with 100 µM H_2O_2. Blank means cells without H_2O_2, CCWPs, CSWPs, and IOUFPs. Data are mean ± SD of at least 3 replicates, $n = 3$, * $p < 0.05$, ** $p < 0.01$, compared to the control group (viability of cells without exposure of particles 100%): (a) significant difference as compared with CCWP between cell CHO and A549 lines at $p < 0.05$; (b) significant difference as compared with CSWP between cell CHO and A549 lines at $p < 0.05$; and (c) significant difference as compared with IOUFP between cell CHO and A549 lines at $p < 0.05$.

However, even trace levels (nM) of cellular and circulating active transition metal ions such as Fe, Cu, Ni, and others present in brake pads appear to be sufficient to catalyze a slow Fenton reaction in vivo. This occurs at physiological H_2O_2 concentrations (0.1–1.0 µM), as demonstrated by Repetto et al. [32]. It is known that, at lower physiological concentrations, H_2O_2 acts as a classical intracellular signaling molecule and regulates kinase-controlled signaling pathways [65]. However, an exposure to IOUFP, which is expected to ionize in the medium, generates concentrations higher than physiological concentrations of H_2O_2. This in turn can have a significant impact on the cellular oxidative stress. The studies [66,67] have shown that the oxidative stress due to an excessive ROS accumulation is a source of IOUFP-induced cytotoxicity.

Given the observed differences in the CCWP and CSWP effects between the CHO and A549 cell lines, the GSH concentration was assessed based on the known relationship between GSH variations, the cellular response to ROS, and cell death. GSH is a reducing agent and is known to catalyze the reduction of H_2O_2, organic hydroperoxides to water, or the corresponding alcohols [28].

GSH, primarily produced intracellularly (85–90%), is the most abundant non-protein thiol in mammalian cells and acts as an important reducing agent and an antioxidant. It scavenges ROS by reducing them and producing oxidized glutathione (GSSG) as a by-product [67,68].

Glutathione in CHO cells was not determined at higher concentrations than the control group under the effect of CCWP suspensions in the studied range of concentrations (Figure 6A).

An exposure of CHO cells to the 10 µg/mL CSWP suspension resulted in a 10% reduction in GSH compared to the control group. However, increasing the CSWP concentration to 40 µg/mL resulted in a 6% increase in the GSH concentration compared to the control group. The subsequent doubling of the CSWP concentration to 80 µg/mL increased the GSH content of the CHO cells to 25% above the control value. A549 cells showed an increased sensitivity to CCWP and exhibited a 17% reduction in the GSH levels at the lowest concentration of 10 µg/mL. This effect was less pronounced at higher concentrations: the

GSH levels increased to 6% and 27% above the control value at 40 and 80 µg/mL for A549 cells, respectively. An exposure of A549 cells to 10 µg/mL CSWP resulted in a 20% reduction in the GSH concentration compared to the control group. However, this effect was only insignificantly reduced with the increasing CSWP concentration.

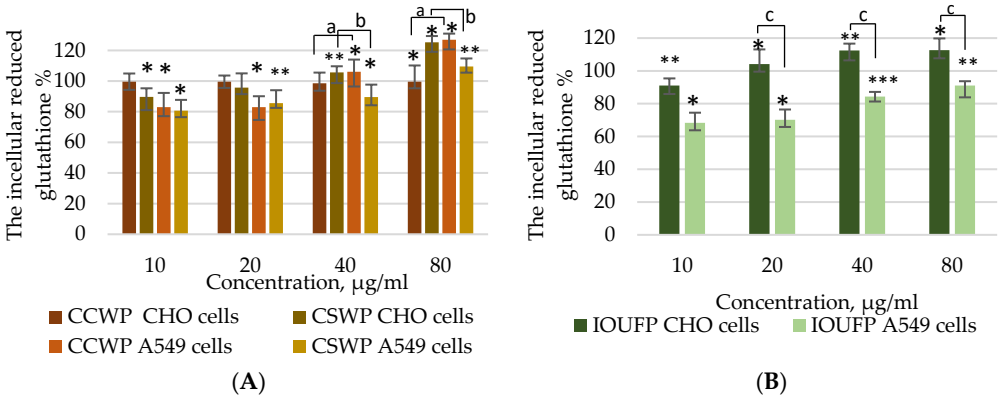

Figure 6. Effect of the CCWP, CSWP (**A**), and IOUFP (**B**) suspension for 24 h on the GSH of CHO and A549 cells. Data are mean ± SD of at least 3 replicates, $n = 3$, * $p < 0.05$, ** $p < 0.01$, *** $p < 0.001$ compared to the control group (viability of cells without exposure of particles 100%): (a) significant difference as compared with CCWP between cell CHO and A549 lines at $p < 0.05$; (b) significant difference as compared with CSWP between cell CHO and A549 lines at $p < 0.05$; and (c) significant difference as compared with IOUFP between cell CHO and A549 lines at $p < 0.05$.

The results of the GSH study for CHO and A549 cells exposed to IOUFP (Figure 6B) correlate with the observed ROS changes (Figure 5B). The data suggest that A549 cells are more sensitive to the IOUFP exposure than CHO cells. In particular, the GSH levels remained higher in CHO cells than for the control group in all cases except for the lowest concentration of 10 µg/mL. In contrast, the GSH content in A549 cells remained below the control value at all concentrations, reaching its lowest value (68% of the control value) at 10 µg/mL and gradually increasing to 91% of the control value at the highest concentration of 80 µg/mL.

While CCWP and CSWP had different effects on the GSH content in CHO and A549 cells, both cell lines showed a trend towards an increased sensitivity to IOUFP, with A549 cells showing a greater reduction in the GSH content at all concentrations.

To assess the oxidative stress-induced membrane as the primary target of CCWP, CSWP, and IOUFP damage, malondialdehyde (MDA) levels were measured, which are a marker of lipid peroxidation (Figure 7A,B). The initiation, which is the first step in the three-step process of lipid peroxidation [69,70], involves the homolytic cleavage of H_2O_2 and organic hydroperoxides (ROOH) catalyzed by transition metals. During the continuous initiation, non-radical compounds are formed while two radicals are neutralized. However, in the presence of transition metal ions, ROOH can produce radicals that reinitiate the lipid peroxidation via redox cycling [30]. Specifically, reduced iron complexes (Fe^{2+}) react with ROOH to form alkoxy radicals, while oxidized iron complexes (Fe^{3+}) react more slowly to form peroxyl radicals. Both radicals can be involved in the continuation of the chain reaction [30]. The products and by-products of lipid peroxidation are considered cytotoxic and can ultimately cause oxidative stress, oxidative damage, and apoptosis [31,71].

An exposure of CHO cells to CCWP showed a concentration-dependent increase in the lipid peroxidation (Figure 7A). This trend was also observed in the experiment with CSWP; however, a pronounced effect was observed when exposed to the 20 mg/mL suspension, when lipid peroxidation of CHO cells was 1.6 times higher than at other concentrations. Increasing the CCWP concentration from 10 to 40 µg/mL resulted in a significant increase from 36 to 61% in the lipid peroxidation of A549 cells. After the A549 cells were exposed to the CSWP suspension, the same trend in the change in the MDA concentration was

maintained. A comparative study of the lipid peroxidation between CHO and A549 cells revealed that CHO cells were generally more sensitive to the CSWP exposure, regardless of the size of the CCWPs.

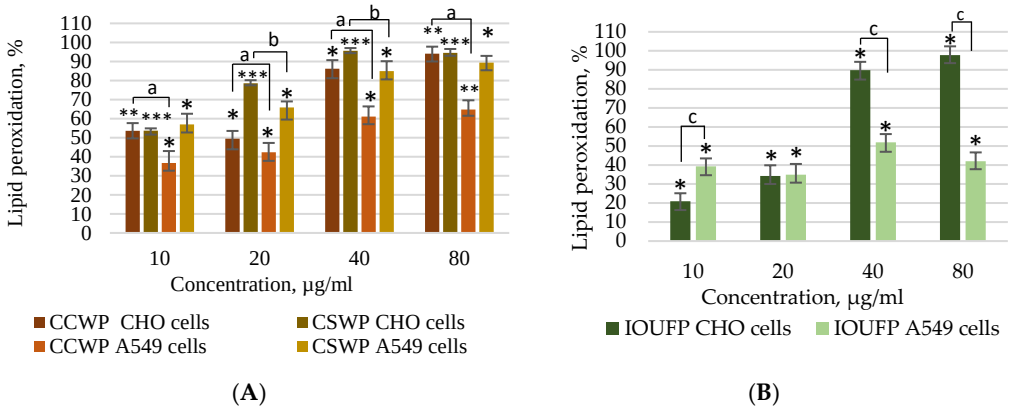

Figure 7. Effect of the CCWP, CSWP (**A**), and IOUFP (**B**) suspensions for 24 h on the lipid peroxidation of CHO and A549 cells. Data are mean ± SD of at least 3 replicates, $n = 3$, * $p < 0.05$, ** $p < 0.01$, *** $p < 0.001$ compared to the control group (viability of cells without exposure of particles 100%): (a) significant difference as compared with CCWP between cell CHO and A549 lines at $p < 0.05$; (b) significant difference as compared with CSWP between cell CHO and A549 lines at $p < 0.05$; and (c) significant difference as compared with IOUFP between cell CHO and A549 lines at $p < 0.05$.

When CHO cells were exposed to the 10 µg/mL IOUFP suspension, the lipid peroxidation reached only about 20% compared to the control value. Doubling the concentration to 20 µg/mL did not lead to a proportional increase in the lipid peroxidation, which reached only 34%. However, at a concentration of 80 µg/mL, the effect of IOUFPs on the lipid peroxidation (Figure 7B) approached that from CCWPs and CSWPs (Figure 7A) and reached about 97%.

The lipid peroxidation was generally lower in A549 cells compared to CHO cells after the exposure to IOUFP suspensions, except for the 10 µg/mL concentration. At all concentrations of the IOUFP suspensions, the lipid peroxidation in A549 cells remained below 52%. The present study revealed that H_2O_2, which can react with redox-active metals such as iron or copper, plays a crucial role in the lipid peroxidation, which agrees with the previously reported results [61,70,72]. This process is particularly important considering that lipids play a crucial role in various biological functions, including as signaling molecules [28].

4. Conclusions

It was found that different cell types with varying membrane morphologies respond differently to the wear particles (CCWPs and CSWPs) and homogeneous IOUFPs.

1. The viability studies using the MTT and Calcein AM assays demonstrated that the A549 cells show reduced susceptibility to CCWPs and CSWPs compared to CHO cells during both short (4 h) and prolonged (24 h) exposures. While 40 or 80 µg/mL IOUFP significantly decreased the CHO cell viability, A549 cells showed a higher sensitivity at lower concentrations. The higher viability observed in the Calcein AM assay may be attributed to the chelating effect of iron.
2. This study highlights the cell-specific nature of the oxidative stress caused by CCWPs, CSWPs, and IOUFPs. A549 cells exhibited higher ROS levels in response to CCWP, whereas the higher IOUFP concentrations reduced ROS in these cells. In contrast, CHO cells displayed increased ROS regardless of the IOUFP concentration. This discrepancy may result from free iron ions released by IOUFPs, which can increase hydrogen peroxide levels, enhancing oxidative stress.

3. In terms of antioxidant response, CCWPs had no effect on the GSH levels in CHO cells but significantly decreased GSH in A549 cells. Both cell types showed changes in GSH that mirrored ROS changes, indicating a higher sensitivity of A549 cells to the IOUFP ultrafine particles.
4. The exposure to CCWPs and CSWPs led to an increase in the lipid peroxidation in both cell types, with a lower sensitivity of A549 cells in general. Notably, IOUFPs caused a moderate lipid peroxidation in CHO cells at the lower concentrations, reaching the levels similar to those of CCWPs and CSWPs at 80 μg/mL.

Author Contributions: Conceptualization, L.T.; methodology, L.T., O.N. and Y.T.; validation, L.T.; investigation, L.T.; writing—original draft preparation, L.T.; writing—review and editing, L.T., L.R., O.N. and Y.T.; visualization, L.T.; supervision, L.R. All authors have read and agreed to the published version of the manuscript.

Funding: This research received no external funding.

Data Availability Statement: Data are contained within the article.

Conflicts of Interest: The authors declare no conflicts of interest.

References

1. Grigoratos, T.; Martini, G. Brake wear particle emissions: A review. *Environ. Sci. Pollut. Res. Int.* **2015**, *22*, 2491. [CrossRef]
2. Thorpe, A.; Harrison, R.M. Sources and properties of non-exhaust particulate matter from road traffic: A review. *Sci. Total Environ.* **2008**, *400*, 270–296. [CrossRef] [PubMed]
3. Harrison, R.M.; Jones, A.M.; Gietl, J.; Yin, J.; Green, D.C. Estimation of the contributions of brake dust, tire wear, and resuspension to nonexhaust traffic particles derived from atmospheric measurements. *Environ. Sci. Technol.* **2012**, *46*, 6523–6529. [CrossRef]
4. Lawrence, S.; Sokhi, R.; Ravindra, K.; Mao, H.; Prain, D.H.; Bull, D.I. Source apportionment of traffic emissions of particulate matter using tunnel measurements. *Atmos. Environ.* **2013**, *77*, 548–556. [CrossRef]
5. Borawski, A. Conventional and unconventional materials used in the production of brake pads—Review. *Sci. Eng. Compos. Mater.* **2020**, *27*, 374–396. [CrossRef]
6. Fahmy, H.M.; Abd El-Daim, T.M.; Mohamed, H.A.E.N.E. Multifunctional nanoparticles in stem cell therapy for cellular treating of kidney and liver diseases. *Tissue Cell* **2020**, *66*, 101371. [CrossRef]
7. Cronholm, P.; Karlsson, H.L.; Hedberg, J.; Lowe, T.A.; Winnberg, L.; Elihn, K.; Wallinder, I.O.; Möller, L. Intracellular uptake and toxicity of Ag and CuO nanoparticles: A comparison between nanoparticles and their corresponding metal ions. *Small* **2013**, *9*, 970–982. [CrossRef]
8. Chang, Y.N.; Zhang, M.; Xia, L.; Zhang, J.; Xing, G. The Toxic Effects and Mechanisms of CuO and ZnO Nanoparticles. *Materials* **2012**, *5*, 2850–2871. [CrossRef]
9. Karlsson, H.; Cronholm, P.; Gustafsson, J.; Möller, L. Copper Oxide Nanoparticles Are Highly Toxic: A Comparison between Metal Oxide Nanoparticles and Carbon Nanotubes. *Chem. Res. Toxicol.* **2008**, *21*, 1726–1732. [CrossRef] [PubMed]
10. Contini, C.; Schneemilch, M.; Gaisford, S.; Quirke, N. Nanoparticle–membrane interactions. *J. Exp. Nanosci.* **2018**, *13*, 62–81. [CrossRef]
11. Lundqvist, M.; Stigler, J.; Elia, G.; Lynch, I.; Cedervall, T.; Dawson, K.A. Nanoparticle size and surface properties determine the protein corona with possible implications for biological impacts. *Proc. Natl. Acad. Sci. USA* **2008**, *105*, 14265–14270. [CrossRef]
12. Lee, J.; Yang, J.; Kwon, S.G.; Hyeon, T. Nonclassical nucleation and growth of inorganic nanoparticles. *Nat. Rev. Mater.* **2016**, *1*, 16034. [CrossRef]
13. Naz, S.; Gul, A.; Zia, M. Toxicity of copper oxide nanoparticles: A review study. *IET Nanobiotechnol.* **2020**, *14*, 1–13. [CrossRef] [PubMed]
14. Heinz, H.; Pramanik, C.; Heinz, O.; Ding, Y.; Mishra, R.K.; Marchon, D.; Flatt, R.J.; Estrela-Lopis, I.; Llop, J.; Moya, S.; et al. Nanoparticle decoration with surfactants: Molecular interactions, assembly, and applications. *Surf. Sci. Rep.* **2017**, *72*, 1–58. [CrossRef]
15. Yun, Y.; Cho, Y.W.; Park, K. Nanoparticles for oral delivery: Targeted nanoparticles with peptidic ligands for oral protein delivery. *Adv. Drug Deliv. Rev.* **2013**, *65*, 822–832. [CrossRef] [PubMed]
16. Fang, R.H.; Jiang, Y.; Fang, J.C.; Zhang, L. Cell membrane-derived nanomaterials for biomedical applications. *Biomaterials* **2017**, *128*, 69–83. [CrossRef]
17. Mohanraj, J.; Chen, Y. Nanoparticles—A Review. *Trop. J. Pharm. Res.* **2006**, *5*, 561–573. [CrossRef]
18. Karlsson, H.L.; Cronholm, P.; Hedberg, Y.; Tornberg, M.; De Battice, L.; Svedhem, S.; Wallinder, I.O. Cell membrane damage and protein interaction induced by copper containing nanoparticles—Importance of the metal release process. *Toxicology* **2013**, *313*, 59–69. [CrossRef]

19. Wang, Z.; Li, N.; Zhao, J.; White, J.C.; Qu, P.; Xing, B. CuO nanoparticle interaction with human epithelial cells: Cellular uptake, location, export, and genotoxicity. *Chem. Res. Toxicol.* **2012**, *25*, 1512–1521. [CrossRef]
20. Hillaireau, H.; Couvreur, P. Nanocarriers' entry into the cell: Relevance to drug delivery. *Cell. Mol. Life Sci.* **2009**, *66*, 2873–2896. [CrossRef] [PubMed]
21. Panariti, A.; Miserocchi, G.; Rivolta, I. The effect of nanoparticle uptake on cellular behaviour: Disrupting or enabling functions? *Nanotechnol. Sci. Appl.* **2012**, *5*, 87–100. [CrossRef]
22. Behzadi, S.; Serpooshan, V.; Tao, W.; Hamaly, M.A.; Alkawareek, M.Y.; Dreaden, E.C.; Brown, D.; Alkilany, A.M.; Farokhzad, O.C.; Mahmoudi, M. Cellular uptake of nanoparticles: Journey inside the cell. *Chem. Soc. Rev.* **2017**, *46*, 4218–4244. [CrossRef]
23. Bouallegui, Y.; Ben Younes, R.; Turki, F.; Mezni, A.; Oueslati, R. Effect of exposure time, particle size and uptake pathways in immune cell lysosomal cytotoxicity of mussels exposed to silver nanoparticles. *Drug Chem. Toxicol.* **2018**, *41*, 169–174. [CrossRef]
24. Lee, J.; Twomey, M.; Machado, C.; Gomez, G.; Doshi, M.; Gesquiere, A.J.; Moon, J.H. Caveolae-Mediated Endocytosis of Conjugated Polymer Nanoparticles. *Macromol. Biosci.* **2013**, *13*, 913–920. [CrossRef]
25. Privalova, L.I.; Katsnelson, B.A.; Loginova, N.V.; Gurvich, V.B.; Shur, V.Y.; Valamina, I.E.; Makeyev, O.H.; Sutunkova, M.P.; Minigalieva, I.A.; Kireyeva, E.P.; et al. Subchronic Toxicity of Copper Oxide Nanoparticles and Its Attenuation with the Help of a Combination of Bioprotectors. *Int. J. Mol. Sci.* **2014**, *15*, 12379–12406. [CrossRef]
26. Gupta, G.; Cappellini, F.; Farcal, L.; Gornati, R.; Bernardini, G.; Fadeel, B. Copper oxide nanoparticles trigger macrophage cell death with misfolding of Cu/Zn superoxide dismutase 1 (SOD1). *Part. Fibre Toxicol.* **2022**, *19*, 33. [CrossRef]
27. Yao, K.; Ge, W. Differential regulation of Kit Ligand A (*kitlga*) expression in the zebrafish ovarian follicle cells—Evidence for the existence of a cyclic adenosine 3′, 5′ monophosphate-mediated binary regulatory system during folliculogenesis. *Mol. Cell. Endocrinol.* **2015**, *402*, 21–31. [CrossRef]
28. Ayala, A.; Muñoz, M.F.; Argüelles, S. Lipid Peroxidation: Production, Metabolism, and Signaling Mechanisms of Malondialdehyde and 4-Hydroxy-2-Nonenal. *Oxid. Med. Cell. Longev.* **2014**, *2014*, 360438. [CrossRef]
29. Reth, M. Hydrogen peroxide as second messenger in lymphocyte activation. *Immunology* **2002**, *3*, 1129–1134. [CrossRef]
30. Halliwell, B.; Gutteridge, J.M. Oxygen toxicity, oxygen radicals, transition metals and disease. *Biochem. J.* **1984**, *219*, 1–14. [CrossRef]
31. Repetto, M.; Semprine, J.; Boveris, A. Lipid Peroxidation: Chemical Mechanism, Biological Implications and Analytical Determination. In *Lipid Peroxidation*; Catala, A., Ed.; IntechOpen: London, UK, 2012. [CrossRef]
32. Franco, R.; Cidlowski, J.A. Glutathione Efflux and Cell Death. *Antioxid. Redox Signal.* **2012**, *17*, 1694–1713. [CrossRef]
33. Mateos, R.; Goya, L.; Bravo, L. Determination of malondialdehyde by liquid chromatography as the 2,4-dinitrophenylhydrazone derivative: A marker for oxidative stress in cell cultures of human hepatoma HepG2. *J. Chromatogr. B Analyt. Technol. Biomed. Life Sci.* **2004**, *805*, 33–39. [CrossRef] [PubMed]
34. Camandola, S.; Poli, G.; Mattson, M.P. The Lipid Peroxidation Product 4-Hydroxy-2,3-Nonenal Increases AP-1-Binding Activity Through Caspase Activation in Neurons. *J. Neurochem.* **2000**, *74*, 159–168. [CrossRef] [PubMed]
35. Esterbauer, H.; Schaur, R.J.; Zollner, H. Chemistry and biochemistry of 4-hydroxynonenal, malonaldehyde and related aldehydes. *Free Radic. Biol. Med.* **1991**, *11*, 81–128. [CrossRef] [PubMed]
36. Esterbauer, H. Estimation of peroxidative damage. A critical review. *Pathol. Biol.* **1996**, *44*, 25–28.
37. Barosova, H.; Chortarea, S.; Peikertova, P.; Clift, M.J.D.; Petri-Fink, A.; Kukutschova, J.; Rothen-Rutishauser, B. Biological Response of an in Vitro Human 3D Lung Cell Model Exposed to Brake Wear Debris Varies Based on Brake Pad Formulation. *Arch. Toxicol.* **2018**, *92*, 2339–2351. [CrossRef]
38. Gasser, M.; Riediker, M.; Mueller, L.; Perrenoud, A.; Blank, F.; Gehr, P.; Rothen-Rutishauser, B. Toxic Effects of Brake Wear Particles on Epithelial Lung Cells In Vitro. *Part. Fibre Toxicol.* **2009**, *6*, 1–13. [CrossRef]
39. Puisney-Dakhli, C.; Oikonomou, E.K.; Tharaud, M.; Sivry, Y.; Berret, J.F.; Baeza-Squiban, A. Effects of Brake Wear Nanoparticles on the Protection and Repair Functions of the Airway Epithelium. *Environ. Pollut.* **2023**, *327*, 121554. [CrossRef]
40. Alves, C.A.; Soares, M.; Figueiredo, D.; Oliveira, H. Effects of Particle-Bound Polycyclic Aromatic Hydrocarbons and Plasticisers from Different Traffic Sources on the Human Alveolar Epithelial Cell Line A549. *Atmos. Environ.* **2023**, *303*, 119736. [CrossRef]
41. Melzi, G.; Nozza, E.; Frezzini, M.A.; Canepari, S.; Vecchi, R.; Cremonesi, L.; Potenza, M.; Marinovich, M.; Corsini, E. Toxicological Profile of PM from Different Sources in the Bronchial Epithelial Cell Line BEAS-2B. *Toxics* **2023**, *11*, 413. [CrossRef]
42. Puisney, C.; Oikonomou, E.K.; Nowak, S.; Chevillot, A.; Casale, S.; Baeza-Squiban, A.; Berret, J.F. Brake Wear (Nano)particle Characterization and Toxicity on Airway Epithelial Cells In Vitro. *Environ. Sci. Nano* **2018**, *5*, 1036–1044. [CrossRef]
43. Zhao, J.; Lewinski, N.; Riediker, M. Physico-Chemical Characterization and Oxidative Reactivity Evaluation of Aged Brake Wear Particles. *Aerosol Sci. Technol.* **2015**, *49*, 65–74. [CrossRef]
44. Tarasiuk, W.; Golak, K.; Tsybrii, Y.; Nosko, O. Correlations between the wear of car brake friction materials and airborne wear particle emissions. *Wear* **2020**, *456–457*, 203361. [CrossRef]
45. *ISO 19007:2018*; Nanotechnologies—In Vitro MTS Assay for Measuring the Cytotoxic Effect of Nanoparticles. International Organization for Standardization: Geneva, Switzerland, 2018; Last reviewed and confirmed 2023.
46. Kamiloglu, S.; Sari, G.; Ozdal, T.; Capanoglu, E. Guidelines for Cell Viability Assays. *Food Front.* **2020**, *1*, 332–349. [CrossRef]
47. Zhao, K.; Li, M.; Zhao, L.; Sang, N.; Guo, L.H. The Identification of the Major Contributors in Atmospheric Particulate Matter to Oxidative Stress Using Surrogate Particles. *Environ. Sci. Nano* **2021**, *8*, 527–542. [CrossRef]

48. Ohkawa, H.; Ohishi, N.; Yagi, K. Assay for Lipid Peroxides in Animal Tissues by Thiobarbituric Acid Reaction. *Anal. Biochem.* **1979**, *95*, 351–358. [CrossRef] [PubMed]
49. Potter, T.M.; Neun, B.W.; Stern, S.T. Assay to Detect Lipid Peroxidation upon Exposure to Nanoparticles. In *Characterization of Nanoparticles Intended for Drug Delivery*; McNeil, S., Ed.; Methods in Molecular Biology; Humana Press: New York, NY, USA, 2011; Volume 697, pp. 299–310. [CrossRef]
50. Boucher, R.C. Regulation of airway surface liquid volume. *J. Clin. Investig.* **2002**, *109*, 863–868. [CrossRef]
51. Giard, D.J.; Aaronson, S.A.; Todaro, G.J.; Arnstein, P.; Kersey, J.H.; Dosik, H.; Parks, W.P. In Vitro Cultivation of Human Tumors: Establishment of Cell Lines Derived From a Series of Solid Tumors. *J. Natl. Cancer Inst.* **1973**, *51*, 1417–1423. [CrossRef]
52. Stearns, R.C.; Paulauskis, J.D.; Godleski, J.J. Endocytosis of Ultrafine Particles by A549 Cells. *Am. J. Respir. Cell Mol. Biol.* **2001**, *24*, 140–150. [CrossRef] [PubMed]
53. Dumont, J.; Euwart, D.; Mei, B.; Estes, S.; Kshirsagar, R. Human cell lines for biopharmaceutical manufacturing: History, status, and future perspectives. *Crit. Rev. Biotechnol.* **2016**, *36*, 1110–1122. [CrossRef]
54. Stach, C.S.; McCann, M.G.; O'Brien, C.M.; Le, T.S.; Somia, N.; Chen, X.; Lee, K.; Fu, H.-Y.; Daoutidis, P.; Zhao, L.; et al. Model-Driven Engineering of N-Linked Glycosylation in Chinese Hamster Ovary Cells. *ACS Synth. Biol.* **2019**, *8*, 2524–2535. [CrossRef] [PubMed]
55. Forest, V.; Pourchez, J. Biological Effects of Brake Wear Particles in Mammalian Models: A Systematic Review. *Sci. Total Environ.* **2023**, *905*, 167266. [CrossRef]
56. Ragelienė, L.; Trečiokaitė, L.; Tučkutė, S. Analysis of Elemental and Mineral Composition of Car Brake Pads. Chemistry and Chemical Technology 2017. Available online: https://www.vdu.lt/ (accessed on 8 July 2024).
57. Shao, X.-R.; Wei, X.-Q.; Song, X.; Hao, L.-Y.; Cai, X.-X.; Zhang, Z.-R.; Peng, Q.; Lin, Y.-F. Independent effect of polymeric nanoparticle zeta potential/surface charge on their cytotoxicity and affinity to cells. *Cell Prolif.* **2015**, *48*, 465–474. [CrossRef]
58. Šatkauskas, S.; Jakštys, B.; Ruzgys, P.; Jakutavičiūtė, M. Different Cell Viability Assays Following Electroporation In Vitro. In *Handbook of Electroporation*; Miklavcic, D., Ed.; Springer: Cham, Switzerland, 2016; pp. 1–16. [CrossRef]
59. Rajeckaitė, V.; Jakštys, B.; Rafanavičius, A.; Maciulevičius, M.; Jakutavičiūtė, M.; Šatkauskas, S. Calcein Release from Cells In Vitro via Reversible and Irreversible Electroporation. *J. Membr. Biol.* **2018**, *251*, 119–130. [CrossRef]
60. Tenopoulou, M.; Kurz, T.; Doulias, P.T.; Galaris, D.; Brunk, U.T. Does the calcein-AM method assay the total cellular 'labile iron pool' or only a fraction of it? *Biochem. J.* **2007**, *403*, 261–266. [CrossRef]
61. Mosmann, T. Rapid Colorimetric Assay for Cellular Growth and Survival: Application to Proliferation and Cytotoxicity Assays. *J. Immunol. Methods* **1983**, *65*, 55–63. [CrossRef]
62. Figliuzzi, M.; Tironi, M.; Longaretti, L.; Mancini, A.; Teoldi, F.; Sangalli, F.; Remuzzi, A. Copper-dependent biological effects of particulate matter produced by brake systems on lung alveolar cells. *Arch. Toxicol.* **2020**, *94*, 2965–2979. [CrossRef] [PubMed]
63. Bielski, B.H.J.; Arudi, R.L.; Sutherland, M.W. A study of the reactivity of HO2/O2− with unsaturated fatty acids. *J. Biol. Chem.* **1983**, *258*, 4759–4761. [CrossRef] [PubMed]
64. Song, Y.K.; Hong, S.H.; Jang, M.; Kang, J.H.; Kwon, O.Y.; Han, G.M.; Shim, W.J. Large Accumulation of Micro-Sized Synthetic Polymer Particles in the Sea Surface Microlayer. *Environ. Sci. Technol.* **2014**, *48*, 9014–9021. [CrossRef] [PubMed]
65. Gough, D.; Cotter, T. Hydrogen peroxide: A Jekyll and Hyde signalling molecule. *Cell Death Dis.* **2011**, *2*, e213. [CrossRef] [PubMed]
66. Hsiao, J.K.; Chu, H.H.; Wang, Y.H.; Lai, C.W.; Chou, T.P.; Hsieh, T.S.; Wang, L.J.; Liu, M.H. Macrophage physiological function after superparamagnetic iron oxide labeling. *NMR Biomed.* **2008**, *21*, 820–829. [CrossRef] [PubMed]
67. Lunova, O.; Syrovets, T.; Röcker, C.; Tron, K.; Nienhaus, U.; Rasche, V.; Mailander, V.; Landfester, K.; Simmet, T. Lysosomal degradation of the carboxydextran shell of coated superparamagnetic iron oxide nanoparticles and the fate of professional phagocytes. *Biomaterials* **2010**, *31*, 9015–9022. [CrossRef] [PubMed]
68. García-Caparrós, P.; De Filippis, L.; Gul, A.; Hasanuzzaman, M.; Ozturk, M.; Altay, V.; Lao, T.M. Oxidative Stress and Antioxidant Metabolism under Adverse Environmental Conditions: A Review. *Bot. Rev.* **2021**, *87*, 421–466. [CrossRef]
69. Yin, H.; Xu, L.; Porter, N.A. Free radical lipid peroxidation: Mechanisms and analysis. *Chem. Rev.* **2011**, *111*, 5944–5972. [CrossRef]
70. Girotti, W. Lipid hydroperoxide generation, turnover, and effector action in biological systems. *J. Lipid Res.* **1998**, *39*, 1529–1542. [CrossRef] [PubMed]
71. Browne, R.W.; Armstrong, D. HPLC analysis of lipid-derived polyunsaturated fatty acid peroxidation products in oxidatively modified human plasma. *Clin. Chem.* **2000**, *46 Pt 1*, 829–836. [CrossRef] [PubMed]
72. Schneider, C.; Boeglin, W.E.; Yin, H.; Porter, N.A.; Brash, A.R. Intermolecular peroxyl radical reactions during autoxidation of hydroxy and hydroperoxy arachidonic acids generate a novel series of epoxidized products. *Chem. Res. Toxicol.* **2008**, *21*, 895–903. [CrossRef]